Computer Simulations of Wavefronts in Drosophila Embryos

Pablo V. Negrón–Marrero*
Department of Mathematics
University of Puerto Rico
Humacao, PR 00791-4300

March, 2013

Abstract

In this paper we describe a model based on mechanical signaling to study the propagation of wavefronts in Drosophila embryos during mitosis. In this model the embryo membrane is modeled using the equations of elasticity for thin membranes, including the effects of external (dipole type) forces and a damping term. After a brief introduction to the equations for thin membranes and mechanical signaling, we describe a finite element scheme for the approximate solution of the resulting diffusion type system of partial differential equations. We present some preliminary results of a computer simulation using the proposed model assuming the embryo membrane is an ellipsoidal shell.

1 Introduction

In early embryos of many species mitosis progresses as a wavefront through the embryo. Some kind of inter–cellular signal regulates the mitotic behavior as the divisions are spatially and temporally organized across the embryo. Such signaling is generally assumed to be biochemical in nature, but there is also a strong mechanical component to mitosis due to the displacements of the chromosomes during division. There are 14 cycles in mitosis. At the beginning of the ninth cycle, all of the nuclei migrate to the shell of the

*pnm@mate.uprh.edu

embryo. The mitosis wavefronts are only observed between cycles 9-13. For a given cycle (of mitosis) in a given embryo, two wavefronts (metaphasic and anaphasic) travel at the same speed. Both wavefronts slow down with cycle, and produce large-scale collective motion of the nuclei. In this paper we use the model proposed in [4] for the early embryo as a mechanically excitable medium, through which mitotic wavefronts can propagate via stress diffusion.

2 Mechanical signaling

We think of the embryo membrane as an ellipsoidal shell in three dimensions. The shell deforms due to three types of forces:

- internal mechanical forces due to the elastic properties of the shell;
- active force dipoles generated by the mitotic spindles;
- passive friction.

If $\mathbf{u}(\mathbf{x}, t)$ represents the displacement vector, then the equations of three dimensional elasticity for the above set of forces are given by:

$$\Gamma \frac{\partial \mathbf{u}}{\partial t} = \operatorname{div} \mathbf{C}[\nabla \mathbf{u}] + \operatorname{div} \left[\sum_{k=1}^{N} g_k(\mathbf{u}) \delta(\mathbf{x} - \mathbf{x}_k) \mathbf{d}_k \otimes \mathbf{d}_k \right], \tag{1}$$

where $\mathbf{C}$ is the *(linear) elasticity tensor* and is given by

$$\mathbf{C}[\nabla \mathbf{u}] = \lambda (\operatorname{tr}(\mathbf{E}))\mathbf{I} + 2\mu \mathbf{E}, \quad \mathbf{E} = \frac{1}{2} \left[\nabla \mathbf{u} + \nabla \mathbf{u}^T \right],$$

with λ, μ characterizing the mechanical properties of the shell. In addition there are initial and boundary conditions that we shall specify later. For details about the structure of the term corresponding to the force dipoles we refer to [1] and [7]. The N above represents the number of nuclei on the shell that might undergo mitosis. We added to the basic dipole type force model the function g_k that serve as a mechanism for "activating" the k–th dipole when certain local condition is satisfied (cf. (11)) which makes equation (1) to be nonlinear in $\mathbf{u}$.

These equations need to be further specialized so that:

i) one can make use of the fact that the shell is very thin compared to its axial dimensions;

ii) the partial derivatives involved have to be put in terms of curvilinear coordinates to make use of the two dimensional character of the shell.

There are several standard models of shells in the literature that result from this two step process. The equations that we shall employ in this work are due to Koiter [5]. We refer to [8] for a justification or derivation of Koiter's equations from the three dimensional theory of nonlinear elasticity.

3 The equations for thin shells: Koiter's equations

The development and notation in this section follows very closely the presentation in [2]. A *parametrization* of a surface $\mathcal{S} \subset \mathbb{R}^3$ consists of a mapping $\boldsymbol{\theta} : \omega \subset \mathbb{R}^2 \to \mathbb{R}^3$ such that $\mathcal{S} = \boldsymbol{\theta}(\omega)$. Let

$$\begin{aligned} \mathbf{a}_\alpha(\underline{\mathbf{y}}) &= \partial_\alpha \boldsymbol{\theta}(\underline{\mathbf{y}}), \quad \alpha = 1,2, \\ \mathbf{a}_3(\underline{\mathbf{y}}) &= \frac{\mathbf{a}_1(\underline{\mathbf{y}}) \times \mathbf{a}_2(\underline{\mathbf{y}})}{\left\| \mathbf{a}_1(\underline{\mathbf{y}}) \times \mathbf{a}_2(\underline{\mathbf{y}}) \right\|}, \end{aligned}$$

be the *covariant basis* at $\boldsymbol{\theta}(\underline{\mathbf{y}}) \in \mathcal{S}$, and let $\{\mathbf{a}^1, \mathbf{a}^2, \mathbf{a}^3\}$ be the corresponding *contravariant basis*, i.e., $\mathbf{a}_i \cdot \mathbf{a}^j = \delta_{ij}$ (Kronecker delta)[1]. Let

$$\begin{gathered} a_{\alpha\beta} = \mathbf{a}_\alpha \cdot \mathbf{a}_\beta, \quad a^{\gamma\tau} = \mathbf{a}^\gamma \cdot \mathbf{a}^\tau, \\ b_{\alpha\beta} = \mathbf{a}^3 \cdot \partial_\beta \mathbf{a}_\alpha, \quad b_\alpha^\beta = a^{\beta\sigma} b_{\sigma\alpha}, \quad \Gamma^\sigma_{\alpha\beta} = \mathbf{a}^\sigma \cdot \partial_\beta \mathbf{a}_\alpha. \end{gathered}$$

The matrix $(a_{\alpha\beta})$ is called the *metric tensor* or *first fundamental form* of $\mathcal{S}$, and $(b_{\alpha\beta})$ is the *second fundamental form* of $\mathcal{S}$. It follows that $(a_{\alpha\beta})(a^{\gamma\tau}) = \mathbf{I}$. The functions $\left\{\Gamma^\sigma_{\alpha\beta}\right\}$ are called the *Christoffel symbols of the second type.*

A deformation of the surface $\mathcal{S}$ is given by a function of the form $\boldsymbol{\theta} + \boldsymbol{\eta}$ where $\boldsymbol{\eta} = \eta_i \mathbf{a}^i : \omega \to \mathbb{R}^3$ is the *displacement deformation vector*. For a given $\boldsymbol{\eta}$, we define covariant and contravariant basis, metric tensors, etc., on the deformed surface:

$$\begin{gathered} \mathbf{a}_\alpha[\boldsymbol{\eta}] = \partial_\alpha(\boldsymbol{\theta} + \boldsymbol{\eta}), \quad a_{\alpha\beta}[\boldsymbol{\eta}] = \mathbf{a}_\alpha[\boldsymbol{\eta}] \cdot \mathbf{a}_\beta[\boldsymbol{\eta}], \quad \text{etc.} \\ b_{\alpha\beta}[\boldsymbol{\eta}] = \frac{1}{\sqrt{a[\boldsymbol{\eta}]}} \partial_{\alpha\beta}(\boldsymbol{\theta} + \boldsymbol{\eta}) \cdot (\mathbf{a}_1[\boldsymbol{\eta}] \times \mathbf{a}_2[\boldsymbol{\eta}]), \quad a[\boldsymbol{\eta}] = \det(a_{\alpha\beta}[\boldsymbol{\eta}]). \end{gathered}$$

[1]Roman indexes run over $1,2,3$ while greek indexes run over $1,2$. We make use of the repeated index notation in which an expression like $p^\alpha \eta_\alpha$ stands for the sum $p^1\eta_1 + p^2\eta_2$, etc..

We can now define the tensors:

$$
\begin{aligned}
G_{\alpha\beta}[\boldsymbol{\eta}] &= \frac{1}{2}\left[a_{\alpha\beta}[\boldsymbol{\eta}] - a_{\alpha\beta}\right], \quad \text{(change in metric)},\\
R_{\alpha\beta}[\boldsymbol{\eta}] &= b_{\alpha\beta}[\boldsymbol{\eta}] - b_{\alpha\beta}, \quad \text{(change in curvature)}.
\end{aligned}
$$

The energy functional associated to a displacement deformation vector $\boldsymbol{\eta} = \eta_i \mathbf{a}^i$ of the shell, is defined now by:

$$
\begin{aligned}
E(\boldsymbol{\eta}) &= \frac{1}{2}\int_\omega \Big[\varepsilon a^{\alpha\beta\sigma\tau} G_{\sigma\tau}[\boldsymbol{\eta}] G_{\alpha\beta}[\boldsymbol{\eta}]\\
&\quad + \frac{\varepsilon^3}{3} a^{\alpha\beta\sigma\tau} R_{\sigma\tau}[\boldsymbol{\eta}] R_{\alpha\beta}[\boldsymbol{\eta}]\Big] j(\underline{\mathbf{y}})\,\mathrm{d}\underline{\mathbf{y}} - \int_\omega p^i \eta_i\, j(\underline{\mathbf{y}})\,\mathrm{d}\underline{\mathbf{y}},
\end{aligned}
$$

where $p^i \mathbf{a}_i$ is the average body force across the thickness of the shell, ε is the shell thickness,

$$
j(\underline{\mathbf{y}}) = \sqrt{a(\underline{\mathbf{y}})}, \quad a(\underline{\mathbf{y}}) = \det(a_{\alpha\beta}(\underline{\mathbf{y}})), \quad \underline{\mathbf{y}} \in \omega,
$$

and

$$
a^{\alpha\beta\sigma\tau}(\underline{\mathbf{y}}) = \frac{4\lambda\mu}{\lambda + 2\mu}\, a^{\alpha\beta}(\underline{\mathbf{y}}) a^{\sigma\tau}(\underline{\mathbf{y}}) + 2\mu\left(a^{\alpha\sigma}(\underline{\mathbf{y}}) a^{\beta\tau}(\underline{\mathbf{y}}) + a^{\alpha\tau}(\underline{\mathbf{y}}) a^{\beta\sigma}(\underline{\mathbf{y}})\right),
$$

are the contravariant components of the elasticity tensor in curvilinear coordinates.

Koiter's nonlinear equations are the Euler–Lagrange equations for $E(\cdot)$. The linearization of these equations about $\boldsymbol{\eta} = \mathbf{0}$ gives the linear Koiter's equations, which are given by [2]:

$$
\begin{aligned}
-\left(n^{\alpha\beta} + b^\alpha_\sigma m^{\sigma\beta}\right)|_\beta - b^\alpha_\sigma (m^{\sigma\beta}|_\beta) &= p^\alpha, \quad \text{in } \omega,\\
m^{\alpha\beta}|_{\alpha\beta} - b^\sigma_\alpha b_{\sigma\beta} m^{\alpha\beta} - b_{\alpha\beta} n^{\alpha\beta} &= p^3 \quad \text{in } \omega,
\end{aligned}
$$

together with some boundary conditions. Here the *covariant derivatives* $t^{\alpha\beta}|_\beta$ and $t^{\alpha\beta}|_{\alpha\beta}$ are given by:

$$
\begin{aligned}
t^{\alpha\beta}|_\beta &= \partial_\beta t^{\alpha\beta} + \Gamma^\alpha_{\beta\sigma} t^{\beta\sigma} + \Gamma^\beta_{\beta\sigma} t^{\alpha\sigma},\\
t^{\alpha\beta}|_{\alpha\beta} &= \partial_\alpha (t^{\alpha\beta}|_\beta) + \Gamma^\sigma_{\alpha\sigma} (t^{\alpha\beta}|_\beta),
\end{aligned}
$$

The $\left\{n^{\alpha\beta}\right\}$ and $\left\{m^{\alpha\beta}\right\}$ are the components of the stress and bending moments with respect to the covariant basis, and are related to the deformation via the *constitutive equations*:

$$
n^{\alpha\beta} = \varepsilon a^{\alpha\beta\sigma\tau} \gamma_{\sigma\tau}[\boldsymbol{\eta}], \quad m^{\alpha\beta} = \frac{\varepsilon^3}{3}\, a^{\alpha\beta\sigma\tau} \rho_{\sigma\tau}[\boldsymbol{\eta}], \tag{2}
$$

where

$$\begin{aligned}
\gamma_{\alpha\beta}[\boldsymbol{\eta}] &= \frac{1}{2}\left[\partial_\beta \eta_\alpha + \partial_\alpha \eta_\beta\right] - \Gamma^\sigma_{\alpha\beta}\eta_\sigma - b_{\alpha\beta}\eta_3, \\
\rho_{\alpha\beta}[\boldsymbol{\eta}] &= \partial_{\alpha\beta}\eta_3 - \Gamma^\sigma_{\alpha\beta}\partial_\sigma\eta_3 - b^\sigma_\alpha b_{\sigma\beta}\eta_3 + b^\sigma_\alpha(\partial_\beta\eta_\sigma - \Gamma^\tau_{\beta\sigma}\eta_\tau) \\
&\quad + b^\tau_\beta(\partial_\alpha\eta_\tau - \Gamma^\sigma_{\alpha\tau}\eta_\sigma) + \left(\partial_\alpha b^\tau_\beta + \Gamma^\tau_{\alpha\sigma}b^\sigma_\beta - \Gamma^\sigma_{\alpha\beta}b^\tau_\sigma\right)\eta_\tau,
\end{aligned}$$

are the linearized change in metric and curvature tensors.

Using the linear Koiter's equations, we get that the shell version of (1), averaging over the thickness of the three dimensional shell like structure, is given by

$$\Gamma\, a^{\beta\alpha}\partial_t\eta_\beta = \left(n^{\alpha\beta} + b^\alpha_\sigma m^{\sigma\beta}\right)|_\beta + b^\alpha_\sigma(m^{\sigma\beta}|_\beta) + p^\alpha, \quad \text{in } \omega, \tag{3a}$$

$$\Gamma\,\partial_t\eta_3 = -m^{\alpha\beta}|_{\alpha\beta} + b^\sigma_\alpha b_{\sigma\beta}m^{\alpha\beta} + b_{\alpha\beta}n^{\alpha\beta} + p^3 \quad \text{in } \omega, \tag{3b}$$

where now the $\{\eta_i\}$ are functions of $(\underline{\mathbf{y}}, t)$. Using the constitutive equations (2), the above equations give a system of three fourth order differential equations for the unknowns $\{\eta_i\}$. However in the numerical scheme that we describe in the next section, we consider the bending moments as unknowns as well. Thus we expand the system above with:

$$\frac{\varepsilon^3}{3}\, a^{\alpha\beta\sigma\tau}\rho_{\sigma\tau}[\boldsymbol{\eta}] = m^{\alpha\beta}, \quad \text{in } \omega. \tag{4}$$

Thus we end up now with a second order system of seven equations for the unknowns $\{\eta_i\}$ and $\left\{m^{\alpha\beta}\right\}$. The expression for $n^{\alpha\beta}$ in (2) is still used in (3a). Also we need to specify the boundary and initial conditions, and the $\{p^i\}$ corresponding to the force dipole moments in (1).

4 Numerical schemes and results

We take the surface $\mathcal{S}$ to be the ellipsoid:

$$\frac{x^2}{a^2} + \frac{y^2}{b^2} + \frac{z^2}{c^2} = 1,$$

which can be parametrized by:

$$\boldsymbol{\theta}(\theta, \phi) = (a\cos\theta\,\sin\phi, b\sin\theta\,\sin\phi, c\cos\phi), \tag{5}$$

where

$$\underline{\mathbf{y}} = (\theta, \phi) \in [0, 2\pi] \times [0, \pi].$$

This mapping is singular at the *poles* given by $\phi = 0, \pi$. Thus for our numerical simulations we work instead with the *punctured* ellipsoid given by (5) with

$$\underline{\mathbf{y}} = (\theta, \phi) \in [0, 2\pi] \times [\kappa, \pi - \kappa] \equiv \omega,$$

where $\kappa \in (0, \pi)$ is small. The covariant and contravariant bases $\{\mathbf{a}_j\}$ and $\{\mathbf{a}^k\}$ can now be computed explicitly. We can now specify the boundary conditions in (3) and (4): the functions $\{\eta_i\}$ and $\{m^{\alpha\beta}\}$ are required to be periodic in θ, and for $\phi = \kappa, \pi - \kappa$ we require that:

$$(n^{\alpha\beta} + b^{\alpha}_{\sigma} m^{\sigma\beta})\nu_\beta = 0, \quad \alpha = 1, 2, \tag{6a}$$

$$m^{\alpha\beta}|_\beta \nu_\alpha = 0, \quad a^{\gamma\delta\alpha\beta}(\partial_\alpha \eta_3)\nu_\beta = 0, \quad \gamma, \delta = 1, 2. \tag{6b}$$

We take as initial conditions that:

$$\eta_i(\cdot, 0) = 0, \quad i = 1, 2, 3, \quad m^{\alpha\beta}(\cdot, 0) = 0, \quad \alpha, \beta = 1, 2. \tag{7}$$

Let $v_i(\underline{\mathbf{y}})\mathbf{a}^i$ and $\{w_{\alpha\beta}(\underline{\mathbf{y}})\}$ be smooth *variations* that are periodic in θ. A lengthy but otherwise elementary calculation shows that the weak form of (3) and (4) subject to (6) is given by:

$$\begin{aligned}
&\frac{\varepsilon^3}{3}\int_\omega (\partial_\alpha \eta_3)\big[a^{\gamma\delta\alpha\beta}(\partial_\beta w_{\gamma\delta}) + \partial_\beta\big(a^{\gamma\delta\alpha\beta}\big)w_{\gamma\delta} + a^{\gamma\delta\alpha\beta} w_{\gamma\delta}\Gamma^{\sigma}_{\sigma\beta}\big] j(\underline{\mathbf{y}})\,\mathrm{d}\underline{\mathbf{y}} \\
&+\frac{\varepsilon^3}{3}\int_\omega a^{\gamma\delta\alpha\beta}\big[\Gamma^{\sigma}_{\alpha\beta}\partial_\sigma\eta_3 + b^{\sigma}_{\alpha} b_{\sigma\beta}\eta_3 - b^{\sigma}_{\alpha}(\partial_\beta \eta_\sigma - \Gamma^{\tau}_{\beta\sigma}\eta_\tau) - b^{\tau}_{\beta}(\partial_\alpha\eta_\tau - \Gamma^{\sigma}_{\alpha\tau}\eta_\sigma) \\
&\quad - \big(\partial_\alpha b^{\tau}_{\beta} + \Gamma^{\tau}_{\alpha\sigma} b^{\sigma}_{\beta} - \Gamma^{\sigma}_{\alpha\beta} b^{\tau}_{\sigma}\big)\,\eta_\tau\big] w_{\gamma\delta}\, j(\underline{\mathbf{y}})\,\mathrm{d}\underline{\mathbf{y}} + \int_\omega m^{\gamma\delta} w_{\gamma\delta}\, j(\underline{\mathbf{y}})\,\mathrm{d}\underline{\mathbf{y}} \\
&+ \int_\omega \big[\Gamma(\partial_t\eta_3)v_3 - m^{\alpha\beta}|_\beta(\partial_\alpha v_3) - \big(b^{\sigma}_{\alpha} b_{\sigma\beta} m^{\alpha\beta} + b_{\alpha\beta} n^{\alpha\beta}\big)v_3\big]\, j(\underline{\mathbf{y}})\,\mathrm{d}\underline{\mathbf{y}} \\
&+ \int_\omega \big[\Gamma\, a^{\beta\alpha}(\partial_t\eta_\beta)v_\alpha + (n^{\alpha\beta} + b^{\alpha}_{\sigma} m^{\sigma\beta})\partial_\beta v_\alpha \\
&- \big(\Gamma^{\alpha}_{\beta\sigma}(n^{\beta\sigma} + b^{\beta}_{\tau} m^{\tau\sigma}) + b^{\alpha}_{\sigma} m^{\sigma\beta}|_\beta\big)v_\alpha\big]\, j(\underline{\mathbf{y}})\,\mathrm{d}\underline{\mathbf{y}} = \int_\omega p^k v_k\, j(\underline{\mathbf{y}})\,\mathrm{d}\underline{\mathbf{y}}
\end{aligned} \tag{8}$$

The right hand side involving the $p^k v_k$ is chosen to be consistent with the forcing term in (1) corresponding to the force dipoles. In particular, taking variations consistent with the *Kirchhoff–Love* assumption in Koiter's model and the vectors $\{\mathbf{d}_1, \ldots, \mathbf{d}_N\}$ in (1) to belong to span $\{\mathbf{a}_1, \mathbf{a}_2\}$, we get that

$$\int_\omega p^k v_k\, j(\underline{\mathbf{y}})\,\mathrm{d}\underline{\mathbf{y}} = -\sum_{k=1}^{N}\int_\omega g_k(\boldsymbol{\eta})\delta(\underline{\mathbf{y}} - \underline{\mathbf{y}}_k) d^{\beta}_{(k)} d^{\alpha}_{(k)}[v_{\beta|\alpha} - b_{\alpha\beta} v_3]\, j(\underline{\mathbf{y}})\,\mathrm{d}\underline{\mathbf{y}}, \tag{9}$$

where $\left\{\underline{\mathbf{y}}_1, \ldots, \underline{\mathbf{y}}_N\right\} \subset \omega$ are the curvilinear coordinates of the force dipoles, that is $\mathbf{d}_k = d^{\alpha}_{(k)} \mathbf{a}_\alpha(\underline{\mathbf{y}}_k)$, $k = 1, \ldots, N$, and

$$v_{\beta|\alpha} = \partial_\alpha v_\beta - \Gamma^\sigma_{\alpha\beta} v_\sigma.$$

Let $\Delta t > 0$ be given, and set $t_i = i\Delta t$, $i \geq 0$. We let $\boldsymbol{\eta}^{(i)} = \eta^{(i)}_j \mathbf{a}^j$ and $m^{\alpha\beta}_{(i)}$ to denote approximations of $\boldsymbol{\eta}(\cdot, t_i)$ and $m^{\alpha\beta}(\cdot, t_i)$ respectively, and

$$n^{\alpha\beta}_{(i)} = \varepsilon a^{\alpha\beta\sigma\tau} \gamma_{\sigma\tau}[\boldsymbol{\eta}^{(i)}].$$

The time derivatives appearing in (8) will be approximated by:

$$\partial_t \eta_j(\cdot, t_i) \approx \frac{\eta^{(i)}_j - \eta^{(i-1)}_j}{\Delta t}, \quad j = 1, 2, 3, \quad i = 1, 2, 3, \ldots.$$

Using this and (9) we have the following time discretized version of the weak form (8):

$$\begin{aligned}
&\frac{\varepsilon^3}{3} \int_\omega (\partial_\alpha \eta^{(i)}_3) \big[a^{\gamma\delta\alpha\beta} (\partial_\beta w_{\gamma\delta}) + \partial_\beta \big(a^{\gamma\delta\alpha\beta}\big) w_{\gamma\delta} + a^{\gamma\delta\alpha\beta} w_{\gamma\delta} \Gamma^\sigma_{\sigma\beta}\big] j(\underline{\mathbf{y}})\, \mathrm{d}\underline{\mathbf{y}} \\
&+ \frac{\varepsilon^3}{3} \int_\omega a^{\gamma\delta\alpha\beta} \big[\Gamma^\sigma_{\alpha\beta} \partial_\sigma \eta^{(i)}_3 + b^\sigma_\alpha b_{\sigma\beta} \eta^{(i)}_3 - b^\sigma_\alpha (\partial_\beta \eta^{(i)}_\sigma - \Gamma^\tau_{\beta\sigma} \eta^{(i)}_\tau) - b^\tau_\beta (\partial_\alpha \eta^{(i)}_\tau - \Gamma^\sigma_{\alpha\tau} \eta^{(i)}_\sigma) \\
&\qquad - \big(\partial_\alpha b^\tau_\beta + \Gamma^\tau_{\alpha\sigma} b^\sigma_\beta - \Gamma^\sigma_{\alpha\beta} b^\tau_\sigma\big)\, \eta^{(i)}_\tau\big] w_{\gamma\delta}\, j(\underline{\mathbf{y}})\, \mathrm{d}\underline{\mathbf{y}} + \int_\omega m^{\gamma\delta}_{(i)} w_{\gamma\delta}\, j(\underline{\mathbf{y}})\, \mathrm{d}\underline{\mathbf{y}} \\
&\qquad + \int_\omega \big[\frac{\Gamma}{\Delta t}\, \eta^{(i)}_3 v_3 - m^{\alpha\beta}_{(i)}|_\beta (\partial_\alpha v_3) - \big(b^\sigma_\alpha b_{\sigma\beta} m^{\alpha\beta}_{(i)} + b_{\alpha\beta} n^{\alpha\beta}_{(i)}\big) v_3\big]\, j(\underline{\mathbf{y}})\, \mathrm{d}\underline{\mathbf{y}} \\
&+ \int_\omega \big[\frac{\Gamma}{\Delta t}\, a^{\beta\alpha} \eta^{(i)}_\beta v_\alpha + (n^{\alpha\beta}_{(i)} + b^\alpha_\sigma m^{\sigma\beta}_{(i)}) \partial_\beta v_\alpha - \big(\Gamma^\alpha_{\beta\sigma} (n^{\beta\sigma}_{(i)} + b^\beta_\tau m^{\tau\sigma}_{(i)}) + b^\alpha_\sigma m^{\sigma\beta}_{(i)}|_\beta\big) v_\alpha\big]\, j(\underline{\mathbf{y}})\, \mathrm{d}\underline{\mathbf{y}} \\
&\qquad\qquad = \int_\omega \Big[\frac{\Gamma}{\Delta t}\, \big(a^{\beta\alpha} \eta^{(i-1)}_\beta v_\alpha + \eta^{(i-1)}_3 v_3\big) \\
&\qquad\qquad - \sum_{k=1}^N g_k(\boldsymbol{\eta}^{(i-1)}) \delta(\underline{\mathbf{y}} - \underline{\mathbf{y}}_k) d^\beta_{(k)} d^\alpha_{(k)} (v_{\beta|\alpha} - b_{\alpha\beta} v_3)\Big]\, j(\underline{\mathbf{y}})\, \mathrm{d}\underline{\mathbf{y}}
\end{aligned} \tag{10}$$

For $\{v_k\}$ and $\{w_{\alpha\beta}\}$ in an appropriate finite element space (continuous piecewise polynomials say) and $\boldsymbol{\eta}^{(i-1)}$, $\left\{m^{\alpha\beta}_{(i-1)}\right\}$ given, one can compute from (10) the approximations $\boldsymbol{\eta}^{(i)}$, $\left\{m^{\alpha\beta}_{(i)}\right\}$. The process is repeated up to a maximum value of time t_{max}. This process was implemented using the package FreeFem++ (cf. [3]).

reference configuration: $\frac{x^2}{a^2} + \frac{y^2}{b^2} + \frac{z^2}{c^2} = 1$	$a = b = 1$, $b = 2.5$, $\kappa = 0.01$
shell thickness	$\varepsilon = 0.01$
elasticity tensor	$\mu = \frac{3}{8}$, $\lambda = 0.25$
dragging coefficient	$\Gamma = 0.01$
FE mesh	approximately 3000 nodes
Number of nuclei (force dipoles)	N=72
Δt	0.05
t_{max}	1 (time units)

Table 1: Parameter values for the numerical simulations.

For the functionals $g_k(\boldsymbol{\eta})$ we use:

$$g_k(\boldsymbol{\eta}) = \begin{cases} \rho, & \text{if } \left\|\boldsymbol{\eta}(\underline{\mathbf{y}}_k)\right\| \geq c_{min}, \\ 0, & \text{otherwise}, \end{cases} \tag{11}$$

where $c_{min}(= 0.01)$ is some minimal "threshold concentration" and $\rho(= 0.02)$ is a measure of the force dipole magnitude. The Dirac delta function is approximated by:

$$\delta(\underline{\mathbf{y}}) \approx M\mathrm{e}^{-K\left\|\underline{\mathbf{y}}\right\|^2},$$

where $K(= 100)$ controls the pulse "localization" and M is a constant to adjust for a unit pulse. The $\mathbf{d}_k$'s in (10) are taken as randomly generated unit vectors tangent to the shell.

The various parameters used in the simulations are shown in Table 1. We show in Figure 1 the initial configuration together with the finite element mesh generated by FreeFem++. In Figure 2 we show the computed deformed configuration of the shell after $t_{max} = 1$ time unit, using 144 forced dipoles uniformly distributed over the shell but with random dipole directions. Two "rings" of dipoles close to the poles of the shell are initially active so the that the time evolution can proceed. In Figure 3 we illustrate some of the dynamics of the process of going from Figure 1 to Figure 2. The coloring in this figure is given by the norm of $\boldsymbol{\eta}$, where "blue" represents a small deformation compared to ''red" which represents a large one. One can see initially the two initial active dipole rings near the poles, and as time goes there is a wavefront of active dipole that moves towards the equator of the shell. In Figure 4 we show part of the dynamics for a simulation with the same parameters as above but with dipole pointing towards the poles of the shell.

5 Comments and conclusions

There are several model equations for thin shells. Some of these, like Koiter's equations, can be rigorously justified as a limiting case of the 3D equations for a shell structure. Although there are several programs for solving thin shell equations, there are little or none for time dependent problems. We need to fine tune parameters in the model to better reflect the biology of the actual phenomena. We need to compute with many more nuclei for realistic results. In particular to measure the speed of propagation of the wavefront. The Drosophila egg is actually filled with a fluid. We need to consider the effects of the interaction between this fluid and the shell membrane.

Acknowledgements: This research was sponsored by the NSF–PREM Program of the UPRH (Grant No. DMR–0934195).

References

[1] Aditi Simha, R. and Ramaswamy, S., Hydrodynamic fluctuations and instabilities in ordered suspensions of self-propelled particles, Physical Review Letters, Vol. 89, No. 5, 2002.

[2] Ciarlet, P. G., An introduction to differential geometry with applications to elasticity, Springer–Verlag, 1st edition, May 22, 2006.

[3] Hecht, F., Pironneau, O., Le Hyaric, A., and Ohtsuka, K., FreeFem++, http://www.freefem.org.

[4] Idema, T., Dubuis, J., Manning, M., Nelson, P., and Liu, A., Wavefront propagation and mechanical signaling in early Drosophila embryos, preprint, 2012.

[5] Koiter, W. T., On the mathematical foundation of shell theory, *Actes, Congrès intern. Math.*, Tome 3, p. 123-130, 1970.

[6] Markow, T. A., Beall, S., and Matzkin, L. M., Egg size, embryonic development time and ovoviviparity in Drosophila species, *J. Evol. Biol.*, 22, 430434, 2009.

[7] Ryan, S. D., Haines, B. M.,Berlyand, L. and Karpeev, D., A kinetic model for semi-dilute bacterial suspensions. (submitted to SIAM MMS), (2012).

[8] Steigmann, D. J., Koiter's shell theory from the perspective of three dimensional nonlinear elasticity, *J. of Elasticity*, 111:91-107, 2013.

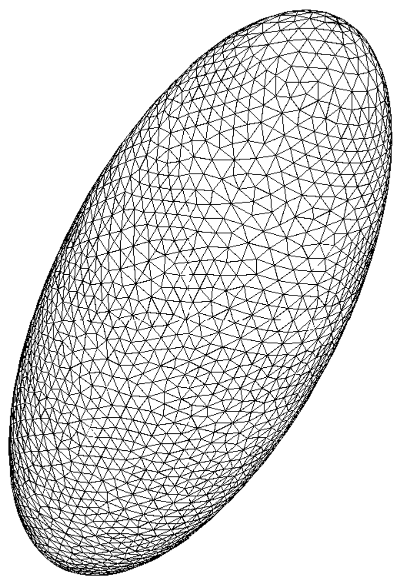

Figure 1: Initial configuration and finite element mesh.

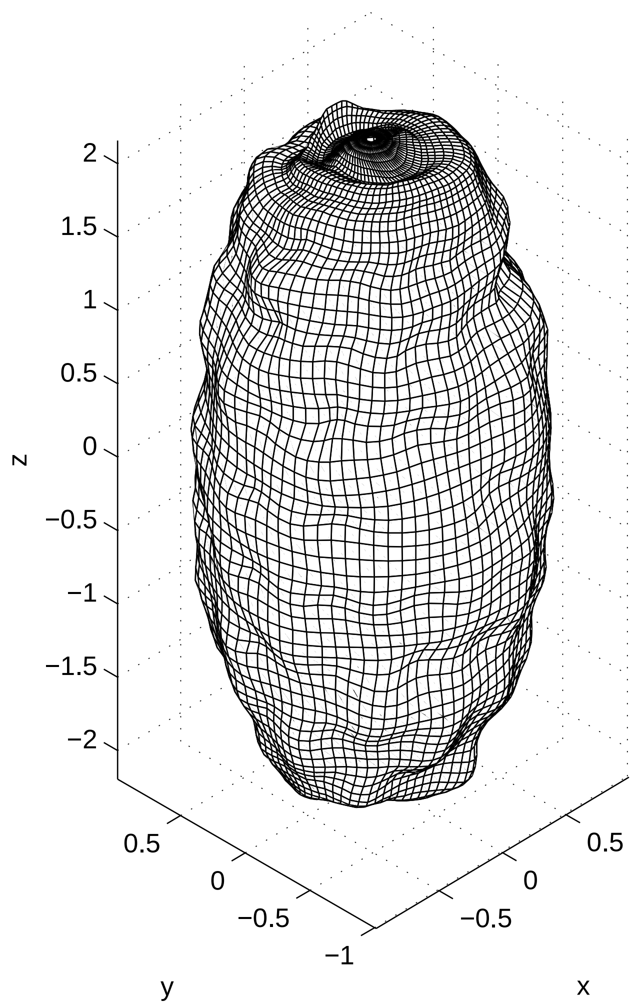

Figure 2: Computed deformation after $t_{max} = 1$ time units with 144 forced dipoles.

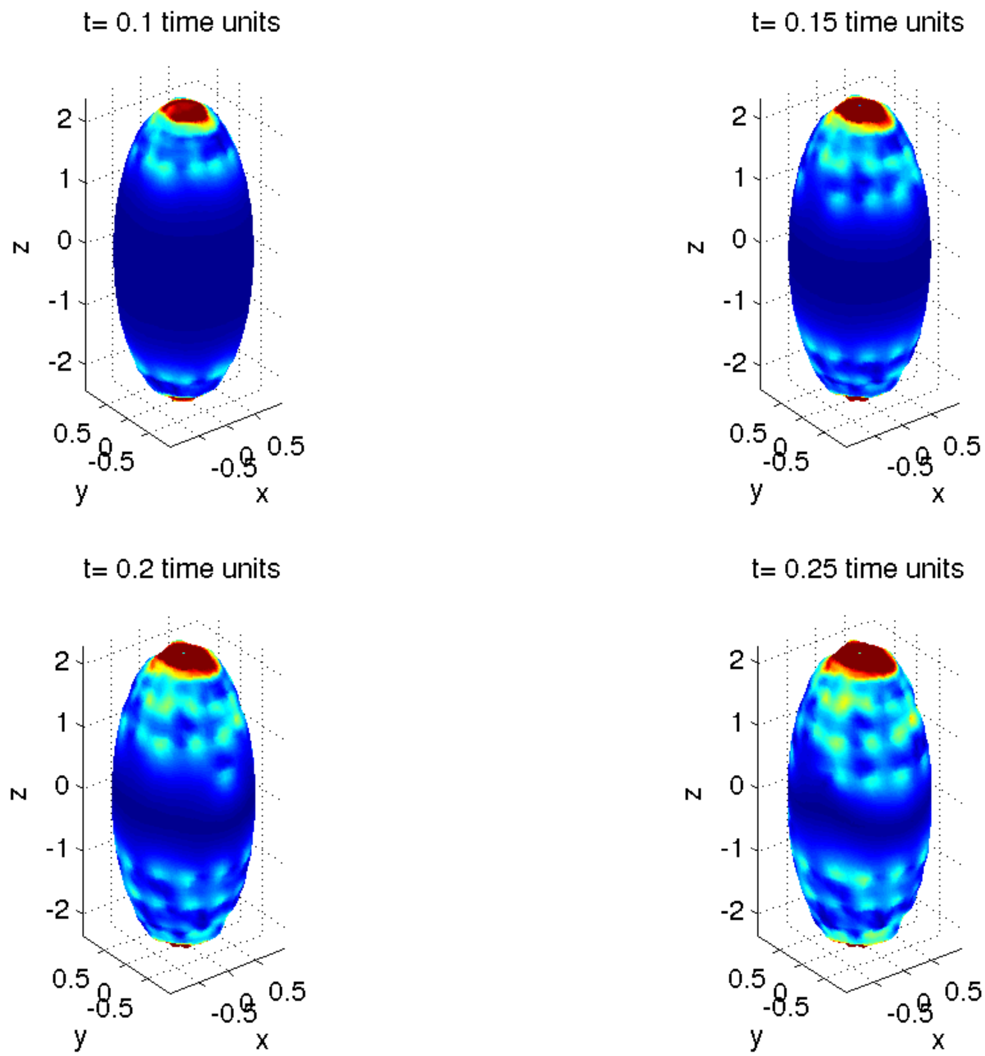

Figure 3: Some of the dynamical process from Figure 1 to 2 showing a wavefront traveling from the poles of the shell to the equator.

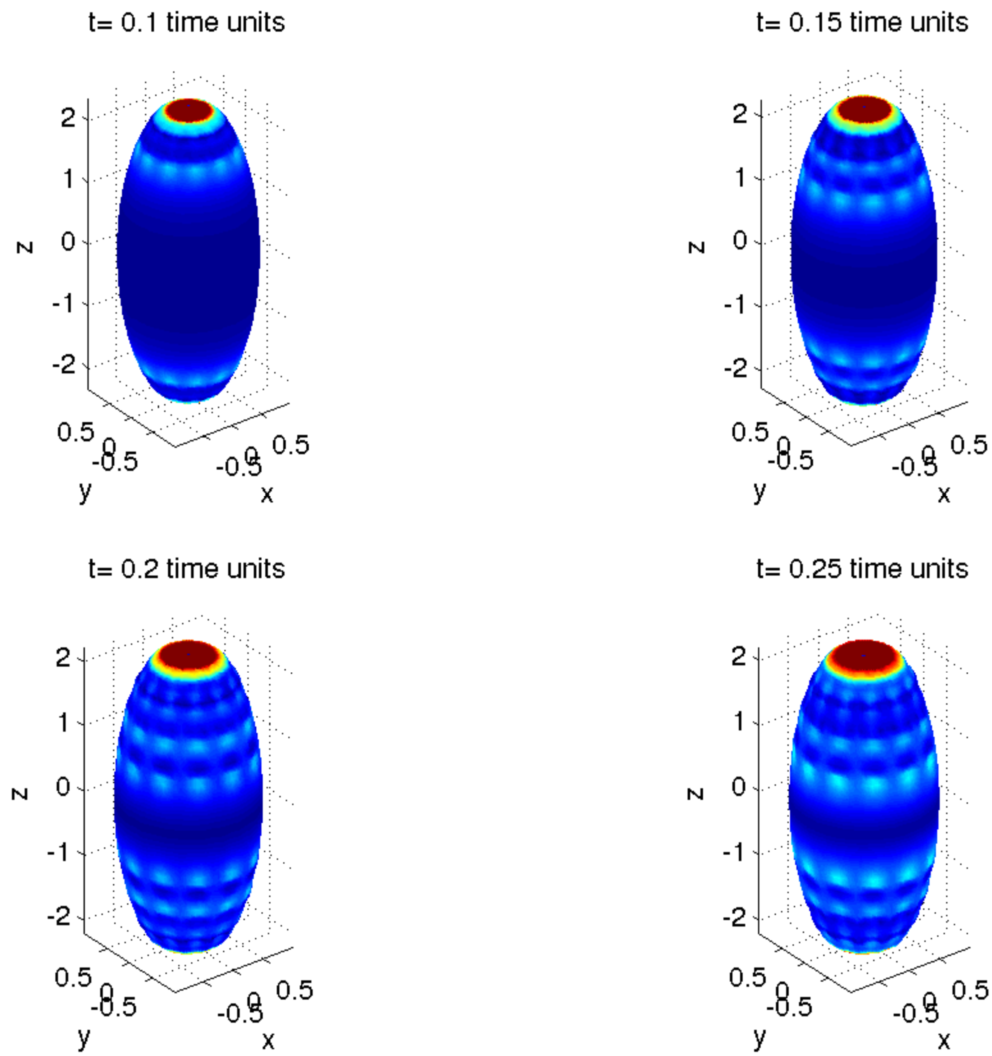

Figure 4: Some of the dynamical process showing a wavefront traveling from the poles of the shell to the equator for dipoles pointing to the poles of the shell.